



Application of plasma-sprayed TiO₂ coatings for industrial (tannery) wastewater treatment

M.C. Bordes^{a,*}, M. Vicent^a, R. Moreno^b, J. García-Montaña^c, A. Serra^c, E. Sánchez^a

^a*Instituto de Tecnología Cerámica (ITC), Universitat Jaume I, Castellón, E-12006 Castellón, Spain*

^b*Instituto de Cerámica y Vidrio (ICV), CSIC, E-28049 Madrid, Spain*

^c*Leitat Technological Center, C/Innovació no. 2, E-08225 Terrassa, Barcelona, Spain*

Received 17 June 2015; received in revised form 10 July 2015; accepted 14 July 2015

Abstract

Fine-structured photocatalytic TiO₂ coatings were deposited by atmospheric plasma spraying (APS) on austenitic stainless steel coupons. One commercial spray-dried nanostructured TiO₂ powder and five spray-dried powders obtained from suspensions containing mixtures of submicrometric and nanometric TiO₂ particles were used as feedstock materials. Coating microstructure and phase composition were characterised using FEG-SEM and XRD techniques. The photocatalytic activity of the coatings was determined by measuring the degradation of methylene blue dye in aqueous solution. The experimental data were observed to follow a pseudo-first-order kinetic. The kinetic constants displayed a clear relationship with coating anatase content.

The photocatalytic decontamination capability of one of these APS coatings was subsequently investigated by treating an industrial tannery wastewater. The photocatalytic experiments with these TiO₂ coated coupons were carried out in a self-designed reactor. Partial degradation of the pollutants was observed, owing to a decrease in Total Organic Carbon (TOC), in addition to a significant decolouration effect, mainly relating to the removal of aromatic organic compounds typically present in tannery wastewater. The results demonstrate the potential use of plasma-sprayed photocatalytic TiO₂ coatings in tannery wastewater treatment.

© 2015 Elsevier Ltd and Techna Group S.r.l. All rights reserved.

Keywords: D. TiO₂; Atmospheric plasma spraying; Photocatalytic activity; Tannery wastewater

1. Introduction

Heterogeneous photocatalysis is an Advanced Oxidation Process (AOP) that allows the complete degradation of pollutants in water and air environments. Titanium dioxide (TiO₂) is the most widely used semiconductor photocatalyst due to its stability, non-toxicity, and relatively low cost [1–3].

As a photocatalyst, TiO₂ is mainly tested in the form of thin films or fine powders, the latter providing better catalytic results. However, the use of particulate TiO₂ entails important environmental and technological drawbacks with regard to recycling and management issues [4,5]. New approaches have therefore been sought for immobilising titania powder in wastewater

treatment and air purification in the last few decades in order to simplify the process and make it competitive. Numerous photocatalytic devices and reactors based on supported photocatalytic coatings have been reported [5,6].

Titanium oxide coatings have long been prepared for many uses by thermal spraying routes, owing to the hardness, wear and corrosion resistance, and biocompatibility of such coatings [7,8]. Extensive research in the last few years has shown that thermal spray techniques, especially atmospheric plasma spraying (APS) can also be used to obtain submicron or nanostructured TiO₂ coatings with effective photocatalytic activity [9–11]. This coating technology also enables preparation of large active coatings that exhibit excellent adhesion to substrates with rather complex shapes [12,13].

Two kinds of phase transitions occur during APS of a given titania feedstock containing anatase phase [11,14]: melting and

*Corresponding author. Tel.: +34 964 64 24 24; fax: +34 964 34 24 25.
E-mail address: carmen.bordes@itc.uji.es (M.C. Bordes).

solidification of the titania phases and solid-state phase transformation from anatase to rutile. For this reason, and in view of the greater photocatalytic efficiency of anatase phase, many studies on such TiO₂ coatings have focused on preserving as much anatase phase as possible in the final coating [9,15,16]. These studies have shown that most of the anatase content comes from the partially melted or unmelted areas that preserve the submicron or nanostructured starting feedstock [17,18]. Consequently, for a given feedstock, the spraying parameters affecting plasma energy input need to be very carefully fine-tuned [14].

Studies on TiO₂ coatings obtained by plasma spraying have assessed their photocatalytic activity, using different procedures. Numerous papers have demonstrated the photocatalytic activity of supported coatings in water solutions using model dyes, in particular methylene blue [19,20], as well as the pink dye Rhodamine B [15], according to more or less standardised methods. Other researchers have preferred the use of model organic or inorganic gaseous molecules such as acetone [21], acetaldehyde [15], ethanol [11], NO_x [22], or even SO₂ [23]. However, no study has been found in which any of these plasma-sprayed photocatalytic coatings have been used to treat wastewater from a real industrial environment. Such an investigation would require construction of a photoreactor capable of holding and testing the supported coatings.

Tannery wastewater represents a serious environmental and technological problem, owing to the large amounts of poorly biodegradable organic chemicals used. At present, most tanneries have a wastewater treatment process that usually consists of three stages: flow homogenisation, dosing coagulants and flocculants; primary decanting to remove suspended solids as well as most of the Chemical Oxygen Demand (COD); and biological treatment with subsequent secondary decanting to remove most of the pollutant content (COD and Biological Oxygen Demand (BOD₅)). However, a tertiary treatment is often still required to refine the COD and remove the colour and/or some organic recalcitrant compounds. As a result, other methods are being increasingly explored as alternatives to classical physico-chemical and biological processes. The literature suggests that photocatalytic treatment as an AOP could be a good option in the near future for organic

matter mineralisation [24]. However, the use of photocatalytic TiO₂ coatings to decontaminate industrial tannery wastewater has not been yet investigated.

The present study was therefore undertaken, first, to develop efficient photocatalytic TiO₂ coatings by the plasma spraying technique (APS), starting from different submicron–nanostructured spray-dried powders. Once the photocatalytic activity in the coatings had been quantified, a reactor was designed to evaluate the application of the developed plasma-sprayed photocatalytic coatings as a tertiary treatment for tannery wastewater.

2. Experimental

2.1. Materials

Nanostructured titania spray-dried powder (NEOXID T101 nano, Millidyne, Finland) was used as commercial feedstock. Five other feedstocks made up of mixtures of a submicron-sized TiO₂ powder and a nano-sized TiO₂ powder were also used. The mixture compositions ranged from 100% submicron-sized particles to 100% nano-sized particles. These starting powders were a submicron-sized, high purity anatase (Titanium (IV) Oxide, Merck, Germany) with a mean particle size of 0.35 µm and a specific surface area of 9.5 m²/g and a commercial nanopowder of titania (AEROXIDE® P25, Degussa-Evonik, Germany) with a mean particle size of 30 nm and a specific surface area of 50 m²/g. P25 nanopowder contains anatase and rutile phases in an approximate 3:1 ratio [25]. The preparation method for each of these five feedstocks consisted, first, of producing a stable aqueous suspension containing the solid mixture and the required amount of dispersant, followed by spray drying of the suspension to obtain the feedstock powder. Further details of the feedstock preparation method can be found elsewhere [18]. Table 1 lists the assigned references as well as some characteristics of the six feedstocks used in this study. Overall, all feedstocks met plasma spray requirements in terms of agglomerate size and density, and powder flowability [26,27].

Table 1

Assigned references as well as some characteristics of the six feedstocks used in this study.

Ref.	Composition	Anatase/rutile ^a (%)	Dry sieving ^b d ₅₀ (µm)	Granule bulk density ^c (kg/m ³)	Hausner ratio ^d	Whiteness index ^e
[1]	100% nano-sized powder	75/25	178	1630	1.12	71.5
[2]	75% nano- + 25% submicron-sized powder	81/19	105	1873	1.09	70.7
[3]	50% nano- + 50% submicron-sized powder	88/13	108	2080	1.11	70.1
[4]	25% nano- + 75% submicron-sized powder	94/6	111	2095	1.13	69.4
[5]	100% submicron-sized powder	100	93	2013	1.14	69.1
C	Commercial spray-dried TiO ₂ powder	80/20	30 ^f	1250	1.18	75.5

^aEstimated from producers data.

^bRecommended value for APS: > 10 µm.

^cRecommended value for APS: > 1700 kg/m³.

^dRecommended value for APS: < 1.25.

^eDetermined with a diffuse reflectance spectrophotometer (ASTM E313-05 standard).

^fDetermined with a diffuse reflectance spectrophotometer (ASTM E313-05 standard).

2.2. Coating deposition and characterisation

Coatings were deposited by APS on metallic substrates (AISI 304) prepared as set out elsewhere [28]. The plasma spray system consisted of a gun (F4-MB, Sulzer Metco, Germany) operated by a robot (IRB 1400, ABB, Switzerland). The deposition was made using argon as primary gas and hydrogen or helium as secondary gas. Helium gas was used to reduce the heat intensity of the plasma jet. The main spraying conditions were as described in previous research [18]. The plasma enthalpy estimate for the H₂ and He plasma conditions used in the present study was 26 ± 2 MJ/kg and 12 ± 1 MJ/kg, respectively [29].

Coating microstructure was analysed on polished cross-sections using a HITACHI S4800 Field Emission Microscope (FEG-SEM). A quantitative crystalline phase composition analysis from X-ray diffraction data (XRD) was conducted based on Rietveld refinement. The XRD patterns were obtained using a Theta-Theta model diffractometer (D8 Advance, Bruker, Germany) with CuK α radiation ($\lambda = 1.54183$ Å). Details of the Rietveld procedure have been reported elsewhere [30,31]. This method was then used to calculate the crystalline phase (anatase and rutile) content (wt%).

Coating photocatalytic activity was determined by assessing the degradation of methylene blue (MB) in aqueous solution. The test evaluated the variation of the MB concentration in a 5 mg/L MB solution in contact with the photocatalytic coating under UV radiation. Irradiation was performed in a chamber using a UVA lamp ($\lambda_{\text{max}} = 370$ nm) with an intensity of 2.5 mW/cm^2 . The test pieces were kept in contact with the MB solution for 30 min in the dark, prior to irradiation, after which the MB concentration was determined at different reaction times. A detailed description of the procedure has been recently reported [16]. Finally, a blank, uncoated sample was tested to evaluate the influence of UV radiation on the decrease in MB concentration achieved by photolysis.

2.3. Photoreactor design and testing

The photocatalytic decontamination capability of the APS coating as tertiary treatment of a tannery wastewater was investigated. An effluent from a Spanish industrial wastewater treatment plant was used, in which tanning industry effluent is mixed with domestic wastewater. The main analytical parameters of this final effluent are detailed in Table 2. The table shows that the resulting wastewater was mainly characterised by high conductivity (salinity content) and high COD values, together with a brownish colour associated with aromatic compounds, as evidenced by the absorbance measured at $\lambda = 254$ nm. As a complementary information on the industrial treatment of the wastewater used in this work, Table 3 collects the evolution of TOC and absorbance at 254 nm, with water treatments (primary and secondary treatments). As it can be seen, after the primary and secondary steps the organic content decreases substantially, but the aromatic compounds content (absorbance) hardly diminishes with the secondary treatment after which most of the organic matter has been removed. For

Table 2

Composition of the studied industrial tannery wastewater.

Parameter	Value
pH	7.3
Conductivity ($\mu\text{S/cm}$)	5240
Turbidity (NTU)	46
Filtered turbidity (NTU)	2.6
Total Suspended Solids (TSS) (mg/L)	34
Total Organic Carbon (TOC) (mg/L)	43.4
Chemical Oxygen Demand (COD) (mg/L)	162
Biochemical Oxygen Demand (BOD5) (mg/L)	37
Dissolved Total Nitrogen (TN) (mg/L)	41
Phenol index (mg/L)	6
Absorbance ($\lambda = 254$ nm)	1.260
Absorbance ($\lambda = 436$ nm)	0.095
Absorbance ($\lambda = 525$ nm)	0.135
Absorbance ($\lambda = 620$ nm)	0.031

Table 3

Evolution of TOC (mg/L) and absorbance at 254 nm in wastewater through the industrial treatment.

	Initial	Primary (physico-chemical)	Secondary (biological)
TOC (mg/L)	1166	911	43.4
Absorbance ($\lambda = 254$ nm)	2.120	1.279	1.260

this reason, a tertiary treatment is necessary to remove this type of pollutants.

The experiments were carried out in a self-designed batch Pyrex glass photoreactor of 2L capacity irradiated by a UVB high-pressure mercury lamp (500 W, 220 V), with a maximum emission at 280–315 nm. Four coated supports ($3 \times 8 \text{ cm}^2$) were located on the inner wall of the reactor (total coated area of approximately 100 cm^2) with a working volume of 770 ml wastewater. The lamp was located concentrically in the reactor in order to ensure homogeneous irradiation of TiO₂. The irradiance on the surface of the coatings was about 12 mW/cm^2 . Coating area, as well as wastewater volume, was optimised after a great number of fine-tuning experiments. For comparative purposes, a commercial photocatalytic sol–gel TiO₂ coating was also tested in the photoreactor under the same conditions as those of the APS coating. The only difference was that the sol–gel coating was applied on glazed ceramic tile supports owing to the better adhesion of the sol–gel coating on the ceramic substrates observed in the tests. The characteristics of this sol–gel material, as well as the procedure for preparing the sol–gel coating, have been previously reported [16]. Fig. 1 shows a picture of the reactor and a scheme of its basic components.

During each experimental run, the solution was vigorously stirred with a magnetic bar to ensure homogenisation and suitable reactant transport to/from the TiO₂ supports. The solution was saturated with oxygen (injected continuously by an oxygen diffuser) in order to accelerate the photocatalytic

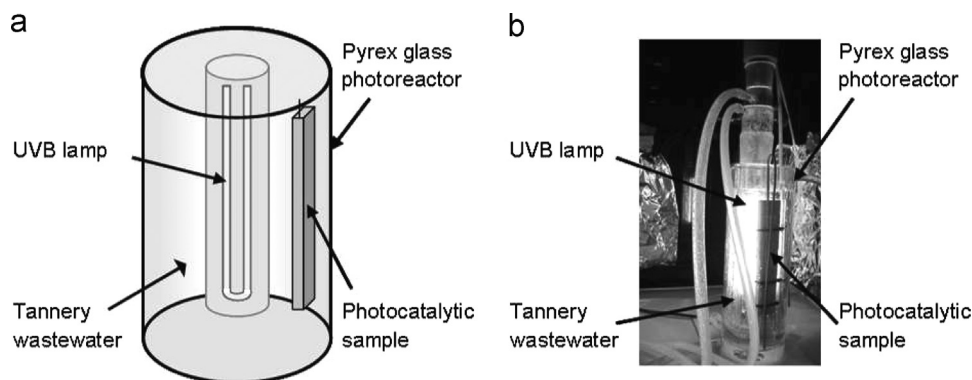


Fig. 1. Photoreactor designed with details of its basic components: (a) scheme, (b) actual picture.

reaction. Solution temperature was kept at 25 °C in every case, both the reactor and the lamp being surrounded with a water circulation jacket connected to an external thermostat. Trials were performed to a maximum of 3 h, aliquots being sampled to measure operational parameters such as TOC, pH, and colour (absorbance). The effect of the photolysis process was determined by conducting an experiment without supports.

Before analysis, all samples withdrawn from the treated solutions were filtered with 0.45 µm PVdF filters to measure the dissolved total organic carbon (TOC). TOC was determined on a Shimadzu V-C DCH TOC analyser, according to standard UNE-EN 1484:1998. Reproducible TOC values, with $\pm 2\%$ accuracy, were obtained by injecting 50 mL aliquots into the TOC analyser. The colour of the wastewater samples was determined using a Hach spectrophotometer by measuring the absorption at 436, 525, and 620 nm wavelengths, as defined in standard UNE-EN ISO 7887. Alternatively, the absorption of samples at 254 nm was also measured in order to monitor the evolution of aromatic species (polyphenol and aromatic intermediates) dissolved in the samples.

3. Results and discussion

3.1. Photocatalytic coating forming and characterisation

The six powders in Table 1 were plasma sprayed, alternately using hydrogen and helium as plasma secondary gas. A total of 12 different types of coatings were thus plasma sprayed. The coating samples were assigned the same references as their powder counterparts (Table 1). For the sake of simplicity, Fig. 2 shows SEM micrographs of the coatings obtained from the intermediate composition feedstock (composition 3: 50% submicron-sized particles/50% nano-sized particles) deposited with hydrogen and helium. No significant differences were observed for the other coatings obtained with H₂ or He. The coatings displayed the typical microstructure of TiO₂ layers deposited from nano- or submicron-structured feedstock reported in the literature [15,30,32,33]. These studies indicate that the coating microstructures are basically made up of two clearly differentiated zones, yielding a bimodal structure. One coating region, which had melted completely (marked M in Fig. 2), consisted mainly of an amorphous titania matrix with recrystallised nanometre-sized grains of rutile. The other

coating region, which had only partially melted (marked PM), largely retained the microstructure of the starting powder. As previously reported [18,30], the unmelted areas were basically made up of nanoparticles or submicron-sized particles that had undergone some degree of sintering.

With regard to the phases present in the final coatings, in all cases (including the commercial powder) the coatings contained variable amounts of rutile and anatase phases with minor contents of Magneli phases as reported elsewhere [34]. Examples of XRD patterns of similar coatings have been reported in previous research [18,30].

Using the Rietveld method, it was found that the anatase content present in the coatings ranged from 2 to 18 wt%, rutile being the major crystalline phase (18 to 58 wt%). The anatase content versus the amount of non-melted areas in the coatings (Fig. 3) has been represented in an x - y - z diagram together with the photocatalytic activity constant (k), in view of the close relationship between this activity and the amount of anatase content in the coating as explained below. The sample references indicated in Table 1 are also shown for coatings deposited with helium. Although data scattering is evident in this figure, the correlation suggests that the preserved anatase particles in the non-melted areas contributed significantly to the anatase content in the coating. The coatings obtained from H₂ (high energy plasma) are located in the bottom left-hand part of the plot: that is, they contain less anatase phase owing to a smaller amount of unmelted areas. In contrast, the coatings obtained with He (low energy plasma) shifted to the top right-hand part of the diagram as a result of the high anatase content associated with the presence of a larger amount of unmelted regions in the coatings. In addition, for the coatings obtained with He the amount of unmelted zones appeared to grow as the submicron-sized particle content in the feedstock increased. This is because, as reported elsewhere, for given plasma spray conditions (plasma energy) the amount and size of the particles inside these unmelted zones depends on the size of the particles making up the feedstock agglomerates (nanoparticles or submicron-sized particles), as well as on other feedstock characteristics such as agglomerate size and density [18,30]. However, the effect of feedstock particle size on the amount of unmelted areas in the final coatings seemed to minimise when a much higher plasma energy (coatings obtained with H₂) was used.

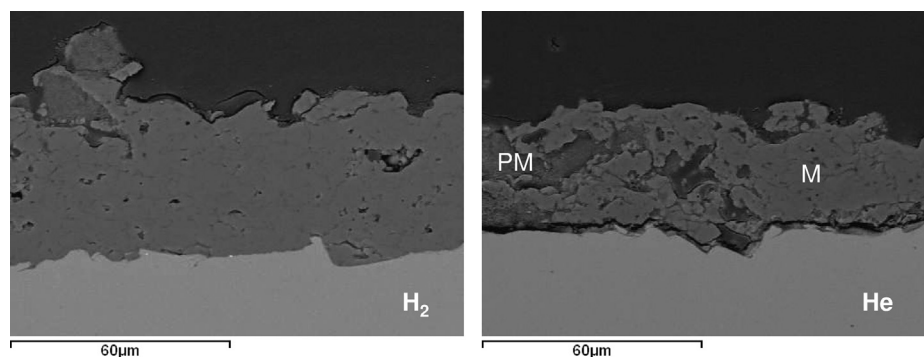


Fig. 2. SEM micrographs of the coatings obtained from the intermediate composition feedstock (composition 3: 50% submicron-sized particles/50% nano-sized particles) deposited with hydrogen and helium.

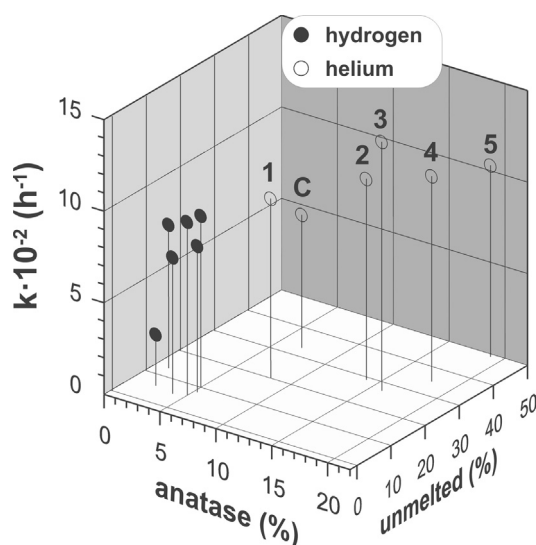


Fig. 3. Plot of anatase content in the coatings versus the amount of non-melted areas and photocatalytic activity constant (k).

In previous research on photocatalytic activity testing with plasma-sprayed coatings, the variation in aqueous MB concentration with time was plotted using a first-order kinetic equation [16]. The kinetic equation fit was used to calculate the photocatalytic activity constant k (h^{-1}). The k values ranged from 2.8 to $13.6 \pm 0.5 \times 10^{-2} \text{ h}^{-1}$ (Fig. 3). A higher k meant a faster degradation rate of the organic MB molecule, i.e. higher photocatalytic activity. Except for one sample, the correlation coefficients were higher than 0.985, indicating reasonably good fit of the experimental data to the kinetic model. To better understand the magnitude of the photocatalytic effect of these coatings, it may be noted that a commercial photocatalytic sol-gel TiO_2 coating tested under similar conditions to those set out above exhibited a rate constant of $5.98 \pm 0.95 \times 10^{-2} \text{ h}^{-1}$ [30].

As indicated above, the x - y - z representation in Fig. 3 also plots k versus anatase content of all obtained coatings. Although the data show significant scattering in the figure, the photocatalytic activity of the coatings for MB degradation displayed a certain correlation with anatase phase content. A higher anatase phase content thus resulted in faster degradation of MB. This finding is consistent with most previous research

[15,19,35]. It also indicates that TiO_2 coatings with a significant photocatalytic activity can be obtained without necessarily using nanostructured feedstocks. This is quite interesting, as the use of submicron-sized particles makes feedstock preparation easier and cheaper. On the other hand, the lack of one single correlation between photocatalytic activity and anatase content is far from unexpected. As the TiO_2 photocatalytic reaction is a surface reaction, the characterisation of surface states with regard to the chemisorbed species, as well as the presence of vacancies and impurities, needs to be addressed. Further research is thus still needed to clarify the role of the coating surface in the photocatalytic activity of plasma spray TiO_2 coatings.

3.2. Wastewater testing with the designed photoreactor

The photocatalytic decontaminating capability of the APS coating was investigated by treating the industrial tannery wastewater described above. The APS coating obtained from the intermediate composition feedstock (composition 3: 50% submicron-sized particles/50% nano-sized particles) was chosen owing to its high photocatalytic constant ($k=11.2 \pm 0.5 \times 10^{-2} \text{ h}^{-1}$), as well as the ease of obtaining a feedstock containing 50 wt% submicron-sized particles.

The pH effect on the photocatalytic degradation of the tannery wastewater was first investigated. According to the literature, the pH effect depends on the nature of the targeted contaminant [36,37]. Moreover, in complex systems containing diverse pollutants such as industrial wastewaters, photocatalytic treatment produces multiple intermediate compounds that can in turn modify their behaviour during treatment as a function of pH. The effect of pH therefore needs to be analysed in terms not only of the degradation of initial pollutants, but also of the compounds produced during treatment by determining global parameters such as TOC or COD [5]. In addition, previous studies [38] have demonstrated that faster photocatalytic degradation of a tannery wastewater can be achieved at low pH. The influence of pH on process efficiency was therefore studied first, working at as-received wastewater pH (pH=7.3) and acidic (pH=2.5) conditions.

Table 4 shows the results of the TOC content in wastewater samples after 1 and 3 h UV treatment at both 2.5 and 7.3 pH.

Table 4
(%) TOC removal in wastewater samples after 1 and 3 h UV photocatalytic and photolytic processes with APS and commercial sol–gel coatings.

Sample	Time (h)	% TOC removal	
		pH=7.6	pH=2.5
No coating	1	4.0	7.4
	3	9.0	21.1
Sol–gel coating	1	5.4	23.7
	3	10.6	33.5
APS coating	1	9.1	9.6
	3	24.2	49.1

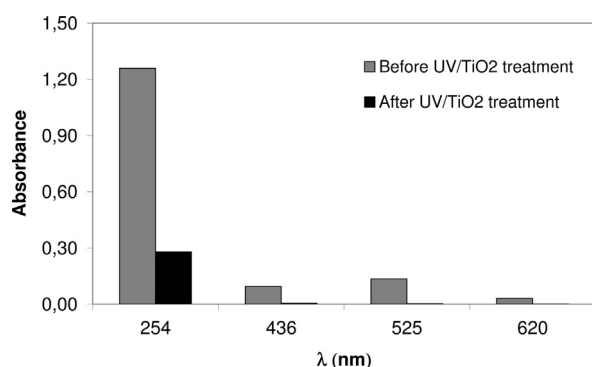


Fig. 4. Absorbance values at 254, 436, 525, and 620 nm wavelengths of untreated and treated wastewater samples after 3 h of photocatalysis with the APS coating (composition 3). pH 2.5.

Only two treated samples were considered, as the kinetic behaviour of the photocatalytic process lay beyond the scope of this first applied study with APS photocatalytic coatings. Photocatalytic experiments were conducted with samples of the APS coating (composition 3) and of the commercial sol–gel coating described above. The results are shown as % TOC decrease with respect to the initial wastewater composition described in Table 2. The findings of the blank experiment (no coatings) to assess the effect of the photolysis are also included in Table 4. It can be observed that a degradation effect associated with photolysis (UV irradiation) occurred in both tested pHs. Moreover, as also reported in the literature, it was confirmed that degradation of the organic compounds by both photolysis and photocatalysis was higher at acidic pH [38]. This behaviour can be related to the effect of pH on the adsorption of the initial or generated organic compounds on the titania surface during UV treatment. The literature indicates that, for example, for a typical anionic black dye used in the tannery industry (Direct Black 38), the optimum pH for the dye to be adsorbed on model photocatalytic powder P25 is 2.5 [39].

The degradation of organic compounds due to the photocatalytic activity was clearly noticeable, as evidenced by a further decrease in TOC in the wastewater treated with the APS coatings when compared with the photolysis effect of the non-photocatalytic blank sample. In addition, the photocatalytic capability of the APS coating was comparable to or even

higher than that of a commercial sol–gel coating tested under the conditions used in this study. This finding agrees with the photocatalytic constants of the APS (composition 3) and commercial coatings indicated above.

Taking into account the best results obtained at acidic pH, the following trials were conducted under pH=2.5. These experiments were carried out to elucidate the effect of the photocatalytic treatment on effluent colour. As indicated above, wastewater colour poses a further problem when managing such effluents treated by conventional practices. The absorbance of the wastewater sample was therefore determined for the APS photocatalytic coating. Testing time in all experiments was 3 h, a sufficiently long time to ensure maximum degradation of organic matter by the photocatalytic effect. Fig. 4 shows the absorbance values at different wavelengths, together with those of the starting (untreated) wastewater detailed in Table 2. As noted, a significant decrease in the absorbance values represents high colour removal due to the photocatalytic effect. In addition, the decolouration effect can largely be attributed to removal of aromatic (phenolic) compounds as evidenced by the strong reduction of absorbance at 254 nm, an aromatic wavelength.

4. Conclusions

TiO₂ coatings were obtained by atmospheric plasma spraying (APS) starting from six different feedstocks: one commercial nano-structured spray-dry powder and five other, self-prepared spray powders obtained from mixtures of nano- and submicron-sized particles. The photocatalytic activity of the coatings was determined by measuring the degradation of methylene blue (MB) dye in aqueous media. In addition, the decontamination capability of the APS coatings was investigated by treating an industrial tannery wastewater. It was confirmed that all resulting coatings were made up of a mixture of rutile (major crystalline phase) and anatase together with a melted TiO₂ matrix. All coatings exhibited the typical APS bimodal microstructure of TiO₂ layers deposited from nano- or submicron-structured feedstock, consisting of unmelted regions which preserved the structure of the feedstock embedded in an amorphous titania matrix. The photocatalytic activity of the coatings, which was comparable to or even better than that of a commercial sol–gel coating, displayed some correlation with the anatase phase content. One of these APS coatings was tested in a self-designed UV photoreactor. The findings showed that there was a clear organic matter mineralisation and colour removal by photocatalysis beyond the photolysis effect under acidic pH. The decreased TOC and colour removal of the resulting effluent evidenced the effectiveness of the developed coatings for photocatalytic treatment of industrial tannery wastewater.

Acknowledgements

This work has been supported by the Spanish Ministry of Economy and Competitiveness (Project MAT2012-38364-C03). The authors also thank the University Jaume I of Castellón for the support provided in project P1-1B2013-69.

References

- [1] A. Fujishima, X. Zhang, D.A. Tryk, Heterogeneous photocatalysis: from water photolysis to applications in environmental cleanup, *Int. J. Hydrog. Energy* 32 (2007) 2664–2672.
- [2] J. Schneider, M. Matsuoka, M. Takeuchi, J. Zhang, Y. Horiuchi, M. Anpo, D.W. Bahnemann, Understanding TiO₂ photocatalysis: mechanisms and materials, *Chem. Rev.* 114 (2014) 9919–9986.
- [3] L. Prieto-Rodríguez, S. Miralles-Cuevas, I. Oller, P. Fernández-Ibáñez, A. Agüera, J. Blanco, S. Malato, Optimization of mild solar TiO₂ photocatalysis as a tertiary treatment for municipal wastewater treatment plant effluents, *Appl. Catal. B: Environ.* 128 (2012) 119–125.
- [4] D.M.A. Alrousan, M.I. Polo-López, P.S.M. Dunlop, P. Fernández-Ibáñez, J.A. Byrne, Solar photocatalytic disinfection of water with immobilised titanium dioxide in re-circulating flow CPC reactors, *Appl. Catal. B: Environ.* 128 (2012) 126–134.
- [5] S. Malato, P. Fernández-Ibáñez, M.I. Maldonado, J. Blanco, W. Gernjak, Decontamination and disinfection of water by solar photocatalysis: recent overview and trends, *Chem. Today* 147 (2009) 1–59.
- [6] M.N. Chong, B. Jin, C.W.K. Chow, C. Saint, Recent developments in photocatalytic water treatment technology: a review, *Water Res.* 44 (2010) 2997–3027.
- [7] R.B. Heimann, Applications of plasma-sprayed ceramic coatings, *Key Eng. Mater.* 122–124 (1996) 399–442.
- [8] R.S. Lima, B.R. Marple, Thermal spray coatings engineered from nanostructured ceramic agglomerated powders for structural, thermal barrier and biomedical applications: a review, *J. Therm. Spray Technol.* 16 (2007) 40–63.
- [9] L. Toma, N. Keller, G. Bertrand, D. Klein, C. Coddet, Elaboration and characterization of environmental properties of TiO₂ plasma sprayed coatings, *Int. J. Photoenergy* 5 (2003) 141–145.
- [10] P. Cübor, V. Stengl, I. Pis, T. Zahoranová, V. Nehasil, Plasma sprayed TiO₂: The influence of power of an electric supply on relations among stoichiometry, surface state and photocatalytic decomposition of acetone, *Ceram. Int.* 38 (2012) 3453–3458.
- [11] M. Bozorgtabar, M. Rahimpour, M. Salehi, M. Jafarpour, Structure and photocatalytic activity of TiO₂ coatings deposited by atmospheric plasma spraying, *Surf. Coat. Technol.* 205 (2011) S229–S231.
- [12] H.R. Khan, H. Frey, R.f. plasma spray deposition of LaMO_x (M Co, Mn, Ni) films and the investigations of structure, morphology and the catalytic oxidation of CO and C₃H₈, *J. Alloy. Compd.* 190 (1993) 209–217.
- [13] F. Ye, A. Ohmori, The photocatalytic activity and photo-absorption of plasma sprayed TiO₂–Fe₃O₄ binary oxide coatings, *Surf. Coat. Technol.* 160 (2002) 62–67.
- [14] J.R. Colmenares-Angulo, V. Cannillo, L. Lusvarghi, A. Sola, S. Sampath, Role of process type and process conditions on phase content and physical properties of thermal sprayed coatings, *J. Mater. Sci.* 44 (2009) 2276–2287.
- [15] F.L. Toma, L.M. Berger, D. Jaquet, D. Wicky, I. Villaluenga, Y.R. de Miguel, J.S. Lindeløv, Comparative study on the photocatalytic behaviour of titanium oxide thermal sprayed coatings from powders and suspensions, *Surf. Coat. Technol.* 203 (2009) 2150–2156.
- [16] E. Bannier, G. Darut, E. Sánchez, A. Denoirjean, M.C. Bordes, M.D. Salvador, E. Rayón, H. Ageorges, Microstructure and photocatalytic activity of suspension plasma sprayed TiO₂ coatings, *Surf. Coat. Technol.* 206 (2011) 378–386.
- [17] G. Bertrand, N. Berger-Keller, C. Meunier, C. Coddet, Evaluation of metastable phase and microhardness on plasma sprayed titania coatings, *Surf. Coat. Technol.* 200 (2006) 5013–5019.
- [18] M.C. Bordes, M. Vicent, A. Moreno, V. López, R. Moreno, M.D. Salvador, R. Benavente, E. Sánchez, Preparation of feedstocks from nano/submicron-sized TiO₂ particles to obtain photocatalytic coatings by atmospheric plasma spraying, *Ceram. Int.* 40 (2014) 16213–16225.
- [19] J. Colmenares-Angulo, S. Zhao, C. Young, A. Orlov, The effects of thermal spray technique and post-deposition treatment on the photocatalytic activity of TiO₂ coatings, *Surf. Coat. Technol.* 204 (2009) 423–427.
- [20] S. Kozerski, F.L. Toma, L. Pawlowski, B. Leupolt, L. Latka, L.M. Berger, Suspension plasma sprayed TiO₂ coatings using different injectors and their photocatalytic properties, *Surf. Coat. Technol.* 205 (2010) 980–986.
- [21] P. Cübor, H. Ageorges, V. Stengl, N. Murafa, I. Pis, T. Zahoranová, V. Nehasil, Z. Pala, Structure and properties of plasma sprayed BaTiO₃ coatings: spray parameters versus structure and photocatalytic activity, *Ceram. Int.* 37 (2011) 2561–2567.
- [22] F.L. Toma, G. Bertrand, S. Begin, C. Meunier, O. Barres, D. Klein, C. Coddet, Microstructure and environmental functionalities of TiO₂-supported photocatalysts obtained by suspension plasma spraying, *Appl. Catal. B: Environ.* 68 (2006) 74–84.
- [23] F.L. Toma, G. Bertrand, D. Klein, C. Coddet, C. Meunier, Nanostructured photocatalytic titania coatings formed by suspension plasma spraying, *J. Therm. Spray Technol.* 15 (2006) 587–592.
- [24] J.M. Herrmann, Heterogeneous photocatalysis: fundamentals and applications to the removal of various types of aqueous pollutants, *Catal. Today* 53 (1999) 115–129.
- [25] T. Ohno, K. Sarukawa, K. Tokieda, M. Matsumura, Morphology of a TiO₂ photocatalyst (Degussa, P-25) consisting of anatase and rutile crystalline phases, *J. Catal.* 203 (2001) 82–86.
- [26] X.Q. Cao, R. Vassen, S. Schwartz, W. Jungen, F. Tietz, D. Stöver, Spray-drying of ceramics for plasma-spray coating, *J. Eur. Ceram. Soc.* 20 (2000) 2433–2439.
- [27] J.A.H. De Jong, A.C. Hoffmann, H.J. Finkers, Properly determine powder flowability to maximize plant output, *Chem. Eng. Prog.* 95 (1999) 25–33.
- [28] E. Sánchez, V. Cantavella, E. Bannier, M.D. Salvador, E. Klyastkina, J. Morgiel, J. Grzonka, A. Boccaccini, Deposition of Al₂O₃–TiO₂ nanostructured powders by atmospheric plasma spraying, *J. Therm. Spray Technol.* 17 (2008) 329–337.
- [29] J. Fazilleau, C. Delbos, V. Rat, J.F. Coudert, P. Fauchais, B. Pateyron, Phenomena involved in suspension plasma spraying Part 1: suspension injection and behavior, *Plasma Chem. Plasma Process.* 26 (2006) 371–391.
- [30] M.C. Bordes, M. Vicent, A. Moreno, R. Moreno, A. Borrell, M.D. Salvador, E. Sánchez, Microstructure and photocatalytic activity of APS coatings obtained from different TiO₂ nanopowders, *Surf. Coat. Technol.* 220 (2013) 179–186.
- [31] R.A. Young, in: *The Rietveld Method*, University Press, Oxford, 1996.
- [32] N. Berger-Keller, G. Bertrand, C. Filatre, C. Meunier, C. Coddet, Microstructure of plasma-sprayed titania coatings deposited from spray-dried powder, *Surf. Coat. Technol.* 168 (2003) 281–290.
- [33] X.Y. Wang, Z. Liu, H. Liao, D. Klein, C. Coddet, Microstructure and electrical properties of plasma sprayed porous TiO₂ coatings containing anatase, *Thin Solid Films* 451–452 (2004) 37–42.
- [34] R.S. Lima, B.R. Marple, From APS to HVOF spraying of conventional and nanostructured titania feedstock powders: a study on the enhancement of the mechanical properties, *Surf. Coat. Technol.* 200 (2006) 3428–3437.
- [35] C.h. Lee, H. Choi, C.h. Lee, H. Kim, Photocatalytic properties of nanostructured TiO₂ plasma sprayed coatings, *Surf. Coat. Technol.* 173 (2003) 192–200.
- [36] U.G. Akpan, B.H. Hameed, Parameters affecting the photocatalytic degradation of dyes using TiO₂-based photocatalysts: a review, *J. Hazard. Mater.* 170 (2009) 520–529.
- [37] J. Sun, X. Wang, J. Sun, R. Sun, S. Sun, L. Qiao, Photocatalytic degradation and kinetics of Orange G using nano-sized Sn(IV)/TiO₂/AC photocatalyst, *J. Mol. Catal. A: Chem.* 260 (2006) 241–246.
- [38] T.P. Sauer, L. Casaril, A.L.B. Oberziner, H.J. José, R.P.M. Moreira, Advanced oxidation processes applied to tannery wastewater containing Direct Black 38-Elimination and degradation kinetics, *J. Hazard. Mater.* 135 (2006) 274–279.
- [39] R.P.M. Moreira, T.P. Sauer, L. Casaril, E. Humeres, Mass transfer and photocatalytic degradation of leather dye using TiO₂/UV, *J. Appl. Electrochem.* 35 (2005) 821–829.